Simvastatin Attenuates Radiation-Induced Murine Lung Injury and Dysregulated Lung Gene Expression

Biji Mathew[1], Yong Huang[2], Jeffrey R. Jacobson[1], Evegeny Berdyshev[1], Lynnette M. Gerhold[3], Ting Wang[1], Liliana Moreno-Vinasco[1], Gabriel Lang[1], Yutong Zhao[1], Chin Tu Chen[3], Patrick J. LaRiviere[3], Helena Mauceri[4], Saad Sammani[1], Aliya N. Husain[5], Steven M. Dudek[1], Viswanathan Natarajan[1], Yves A. Lussier[2], Ralph R. Weichselbaum[4]*, and Joe G. N. Garcia[1]*

[1]Section of Pulmonary and Critical Care Medicine and [2]Section of Genetic Medicine, Department of Medicine, University of Chicago, Chicago, Illinois; Departments of [3]Radiology, [4]Radiation Oncology, and [5]Pathology, Pritzker School of Medicine, University of Chicago, Chicago, Illinois

Novel therapies are desperately needed for radiation-induced lung injury (RILI), which, despite aggressive corticosteroid therapy, remains a potentially fatal and dose-limiting complication of thoracic radiotherapy. We assessed the utility of simvastatin, an anti-inflammatory and lung barrier–protective agent, in a dose- and time-dependent murine model of RILI (18–(25 Gy). Simvastatin reduced multiple RILI indices, including vascular leak, leukocyte infiltration, and histological evidence of oxidative stress, while reversing RILI-associated dysregulated gene expression, including p53, nuclear factor–erythroid-2–related factor, and sphingolipid metabolic pathway genes. To identify key regulators of simvastatin-mediated RILI protection, we integrated whole-lung gene expression data obtained from radiated and simvastatin-treated mice with protein–protein interaction network analysis (single-network analysis of proteins). Topological analysis of the gene product interaction network identified eight top-prioritized genes (Ccna2a, Cdc2, fcer1 g, Syk, Vav3, Mmp9, Itgam, Cd44) as regulatory nodes within an activated RILI network. These studies identify the involvement of specific genes and gene networks in RILI pathobiology, and confirm that statins represent a novel strategy to limit RILI.

Keywords: radiation pneumonitis; lung vascular permeability; simvastatin; gene dysregulation; protein–protein interaction

Radiation-induced lung injury (RILI) is a disabling and potentially fatal, dose-limiting toxicity of thoracic radiotherapy for lung cancer, breast cancer, lymphoma, thymoma, esophageal cancer (1), and total body radiation (2). Although understanding of RILI (or radiation pneumonitis) is limited, RILI is characterized by a subacute course developing over 12–20 weeks, and numerous risk factors have been identified, including the overall radiation dose, daily dose increment, volume of irradiated lung, various comorbidities, and unknown genetic factors (3). Furthermore, RILI may be self-limited, or may progress to overt lung injury associated with significant morbidity or death (4).

RILI is associated with increased generation of reactive oxygen and nitrogen species, secretion of inflammatory cytokines and chemokines, and inflammatory cell recruitment into the lung parenchyma. The molecular basis of RILI, however, remains enigmatic and controversial, which has impeded the successful identification of novel therapeutic targets. To date, therapeutic strategies have largely been designed to ameliorate the acute effects of radiation via neutralizing proinflammatory cytokines or attenuating inflammatory cell infiltration (5). The pluripotential nature of these cytokines and multifaceted signaling pathways complicate their utility as viable targets. Moreover, corticosteroid therapy, commonly used for RILI, suffers from limited efficacy, serious side effects, and the potential for fatal "recall" pneumonitis when abruptly discontinued (6). Alternative treatment strategies, such as anticoagulation or angiotensin-converting enzyme inhibitors, have failed to provide compelling clinical benefit (7).

The pathways regulating vascular and alveolar permeability, intimately involved in the pathophysiology of acute inflammatory lung injury (8), and substantially affected in RILI, represent a potentially novel pathway for targeting RILI. Thoracic radiation perturbs both alveolar epithelium and vascular endothelium (9), resulting in loss of junctional integrity, increased permeability, and physiologic derangement (10). We hypothesized that lung barrier dysfunction may represent a final common pathway that mediates both acute lung injury and subacute RILI. We speculated that statins, a class of 3-hydroxy-3-methylglutaryl–coenzyme A reductase inhibitors, may represent a novel RILI therapy, as this class of drugs exerts potent pleiotropic anti-inflammatory, antithrombotic, and immunomodulatory properties unrelated to lowering cholesterol (11), and have proven to be effective in rodent models of acute lung injury (12).

In the present study, we established a dose- and time-dependent murine model of RILI, and assessed simvastatin as a potential therapeutic intervention. Simvastatin treatment was associated with both an attenuation of lung injury, as assessed by vascular leak, leukocyte infiltration, and histological evidence of oxidative stress, as well as the reversal of radiation-induced dysregulated lung gene expression. Moreover, we demonstrate that computational analysis of key network features linked to lung tissue gene expression analysis allows efficient prioritization of key protein and cellular signals, and discloses genes specifically associated with radiation responses.

MATERIALS AND METHODS

Detailed methods are provided in the online supplement.

Animals

C57BL/6J mice (8- to 10-wk-old; Jackson Labs, Bar Harbor, ME) were used for all studies in accordance with the University of Chicago Institutional Animal Care and Use Committee guidelines.

Radiation Exposure and Simvastatin Treatment

Mice were anesthetized with ketamine (100 mg/kg) and acepromazine (1.5 mg/kg) before single-dose irradiation. In separate experiments,

(*Received in original form March 24, 2010 and in final form April 16, 2010*)

* These authors are co-senior authors of this work.

This work was supported by National Institutes of Health grant HL 58,064 (J.G.N.G., V.N., S.M.D.), and by the Ludwig Cancer Foundation (R.R.W.).

Correspondence and requests for reprints should be addressed to Joe G. N. Garcia, M.D., Vice Chancellor for Research, University of Illinois at Chicago, 1737 West Polk Street, 305D AOB, Chicago, IL 60612-7227. E-mail: jggarcia@uic.edu

This article has an online supplement, which is accessible from this issue's table of contents at www.atsjournals.org

Am J Respir Cell Mol Biol Vol 44. pp 415–422, 2011
Originally Published in Press as DOI: 10.1165/rcmb.2010-0122OC on May 27, 2010
Internet address: www.atsjournals.org

mice were treated with 10 mg/kg simvastatin (Sigma, St. Louis, MO) via intraperitoneal injection three times per week beginning 1 week before irradiation and continuing up to 6 weeks after irradiation.

Bronchoalveolar Lavage Fluid Collection

Bronchoalveolar lavage (BAL) was performed on animals with 1 ml of Hank's buffered saline solution, as we have previously described (13).

Microvascular Permeability Assays

BAL protein concentrations were determined by a colorimetric BCA Bicinchonic Acid assay. Albumin concentrations in the BAL at 1:1,000 and 1:100 dilutions, respectively, were quantitated by ELISA (Bethyl Labs, Montgomery, TX).

Cytokine and Chemokine Assays

To measure cytokines and chemokines, the BAL fluid was assayed with a Bioplex mouse cytokine kit (Bio-Rad, Hercules, CA), in accordance with the manufacturer's instructions.

Evans Blue Dye Extravasation in Lung Tissues

Evans blue dye (EBD) (5 mg/kg) extravasation into lung tissue was performed, as we previously described (14). The EBD concentration is expressed as micrograms per gram of wet weight of lung tissue.

FMT Imaging

ViSen FMT (ViSen Medicals, Bedford, MA) was used for animal imaging. Angiosense^{680} NIR probe (ViSen Medicals) was used to visualize and quantify changes in lung permeability. Mice were injected (intravenously) with the probe (2 nM) at 6 weeks after irradiation and imaged 24 hours afterwards.

Lung Histology and Immunohistochemistry

Lungs were inflated to 30 cm H_2O with 10% formalin for histological evaluation by hematoxylin and eosin staining as we have previously described (15, 16).

RNA Isolation

Total RNA was extracted from lungs using TRIzol reagent (Invitrogen, Carlsbad, CA) and RNeasy kit (Qiagen, Valencia, CA), as we have previously described (15, 16), and was used to synthesize double-stranded cDNA using the One-Cycle DNA Synthesis Kit (Affymetrix, Santa Clara, CA). Biotin-labeled antisense cRNA was then generated and hybridized to the Affymetrix Mouse Genome 430 2.0 Array, as described in the Affymetrix GeneChip protocol (Affymetrix, Santa Clara, CA).

Oligonucleotide Array Analysis

Arrays were normalized and processed using Bioconductor GCRMA package (http://www.bioconductor.org/help/bioc-views/release/bioc/html/gcrma.html). To identify differentially expressed genes, two group comparisons were conducted using significance analysis of microarrays (17). Gene filtering parameters and results are summarized in Table E1 in the online supplement. Data have been submitted to the Gene Expression Omnibus repository of the National Center for Biotechnology Information (GSE14431).

Detailed methods for the identification of gene ontology (GO) categories enriched with dysregulated genes and ingenuity pathway analysis are provided in the online supplement.

Quantitative RT-PCR

Quantification of select transcripts was performed by TaqMan real-time RT-PCR assays and 7900HT Fast Real-time PCR system (Applied Biosystems, Foster City, CA).

Statistical Analysis

Two-way ANOVA was used to compare the means of data from different experimental groups with a Bonferroni test performed *post hoc*. Differences between groups were considered significant with a P value less than 0.05. Results are expressed as means (±SE).

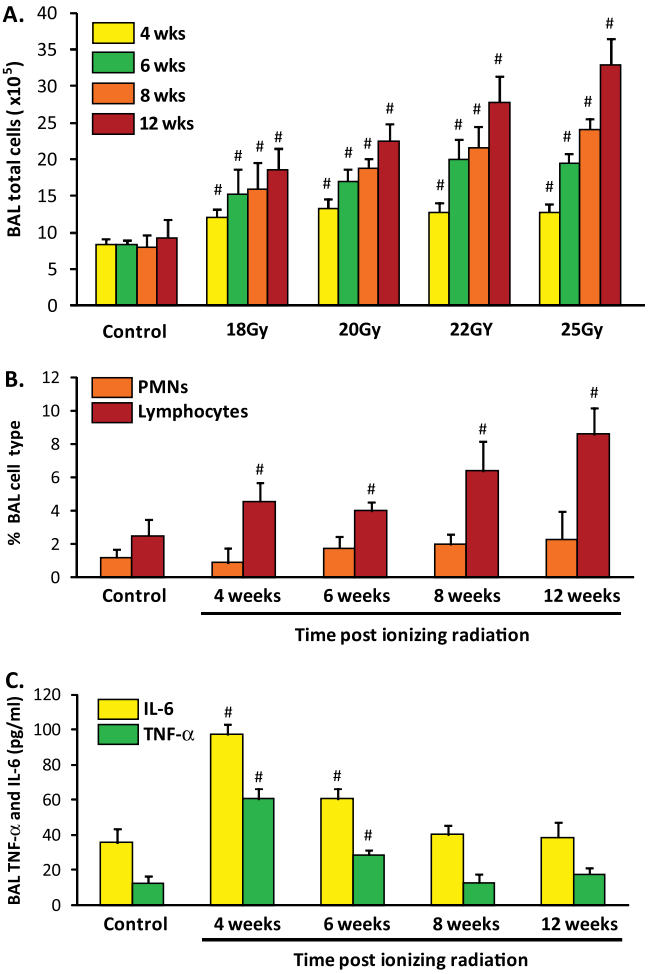

Figure 1. Bronchoalveolar lavage (BAL) cell counts and cytokine expression in a preclinical murine model of radiation-induced lung injury (RILI). (*A*) Thoracic radiation (18–25 Gy) is associated with dose- and time-dependent effects on murine BAL total cell counts. BAL cellularity was not altered before 6 weeks, whereas significant increases in BAL cells was observed at all radiation levels by 12 weeks after irradiation (n = 10 animals/experimental group; $^{\#}P < 0.01$ compared with control). Macrophages represent the dominant cell type (>80%) in each BAL sample, with marked expansion of this cell population in BAL at 12 weeks (25 Gy; data not shown). (*B*) A significant increase in the percentage of BAL lymphocytes (10–20%; $^{\#}P < 0.01$ compared with controls) was noted at 4–12 weeks after irradiation (25 Gy), whereas BAL neutrophil counts were not significantly increased in irradiated mice at any time point. (*C*) Time-dependent effects of radiation are shown with respect to BAL levels of IL-6 and TNF-α in murine RILI. Mice received a single dose of radiation (25 Gy) or mock irradiation to the thorax, and were longitudinally followed (4, 6, 8, and 12 wk). Significant increases in IL-6 and TNF-α relative to controls were observed at 4 and 6 weeks, suggesting an early role of these cytokines in barrier dysfunction (n = 4 animals/experimental group; $^{\#}P < 0.01$). PMN, polymononuclear leukocytes.

RESULTS

Lung Radiation Induces Inflammation and Increased Vascular Leak

To initially characterize a murine model of RILI, female C57BL/6 mice were exposed to a single dose of whole-thoracic radiation (18–25 Gy), and indices of lung inflammation and vascular permeability assessed at intervals of 4, 6, 8, and 12 weeks.

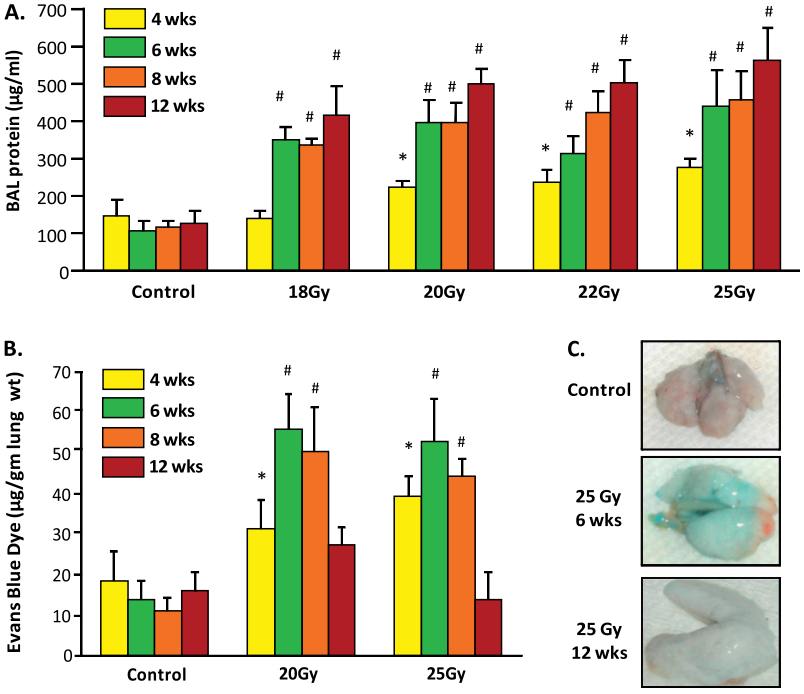

Figure 2. Assessment of increased vascular permeability in murine RILI. (*A*) Thoracic radiation (18–25 Gy) induces dose- and time-dependent effects on murine lung vascular leak. Irradiated mice exhibit significantly increased BAL protein at 6 weeks, with values that peaked at 12 weeks ($n = 7$ animals per experimental group; $^{*}P < 0.05$ and $^{\#}P < 0.01$ compared with respective controls). (*B*) Dose- and time-dependent effects of radiation were also observed with respect to Evans blue dye (EBD) leakage. Significantly increased EBD lung tissue extravasation occurred in irradiated animals (20 and 25 Gy) 6–8 weeks after irradiation ($n = 4$; $^{*}P < 0.05$, $^{\#}P < 0.01$). (*C*) Colorimetric increases are apparent in EBD extravasation as a measure of lung vascular leak after exposure to 25 Gy thoracic radiation.

Irradiated mice demonstrated significant time-dependent increases in levels of BAL total cell counts (Figure 1A), with alveolar macrophages representing the dominant BAL cell type (>85%, with this percentage unchanged with radiation), although the percentage of BAL lymphocytes significantly increased at 8 and 12 weeks after irradiation (Figure 1B). BAL neutrophils (representing <1% of all cells) were not significantly increased at any time point. Companion studies identified significant time-dependent increases in inflammatory markers after radiation, including IL-6 and TNF-α measured in BAL fluid (Figure 1C). In contrast to BAL cell counts, these studies revealed an early increase in BAL cytokines at 4 weeks that then progressively declined and returned to basal levels by 8 weeks.

Irradiated mice demonstrated significant dose- and time-dependent increases in alveolar permeability with progressive increases in BAL protein (Figure 2A), beginning at 2 weeks and sustained throughout the 12-week period. Radiation-mediated increases in the extravasation of intravenously delivered EBD into the lung interstitium, a surrogate marker for vascular permeability (14), peaked at 6 weeks and returned to control levels by 12 weeks (Figures 2B and 2C), suggesting differential susceptibilities of alveolar and lung vascular barriers to thoracic radiation.

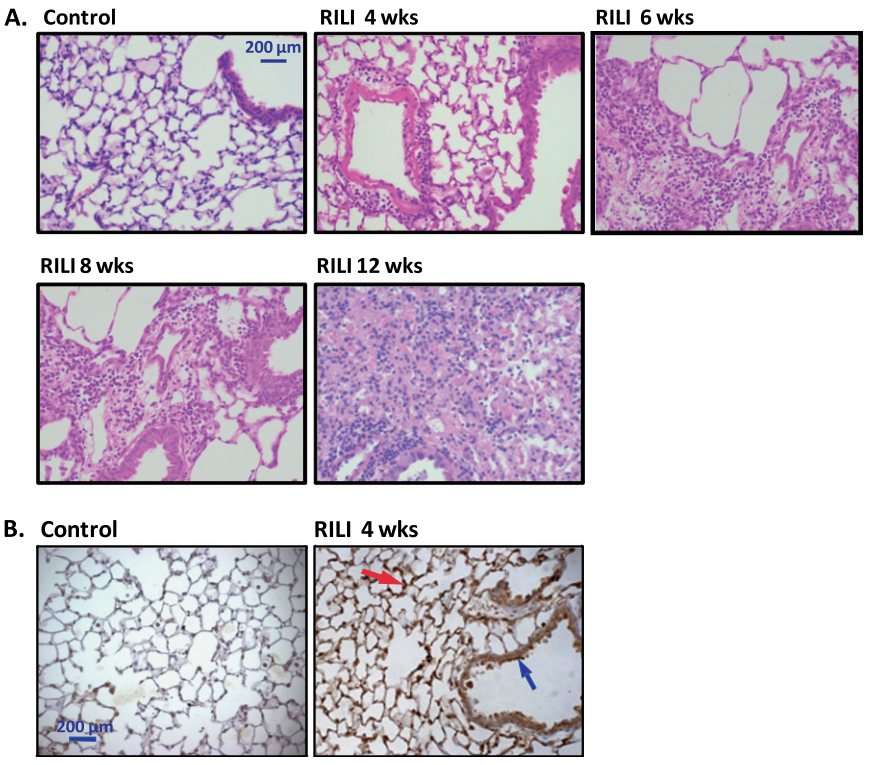

Figure 3. Lung histology and nitrotyrosine expression in murine RILI. (*A*) Hematoxylin and eosin staining of murine lung sections are shown. Compared with control lungs, considerable damage to type I pneumocytes was evident at 4 weeks after irradiation (25 Gy), without visible edema and inflammation. Lungs from mice at 6 weeks after irradiation exhibited modest alveolar flooding and inflammatory foci in scattered areas, with perivascular clustering of inflammatory cells prominent at 8 and 12 weeks. (*B*) Immunohistochemical localization of nitrotyrosine reveals radiation-induced increases in the lungs of exposed mice. Compared with controls, strong immunoreactivity of nitrotyrosine at 4 weeks after irradiation was observed in the alveolar epithelium (*red arrow*), pneumocytes, and airway epithelium (*blue arrow*).

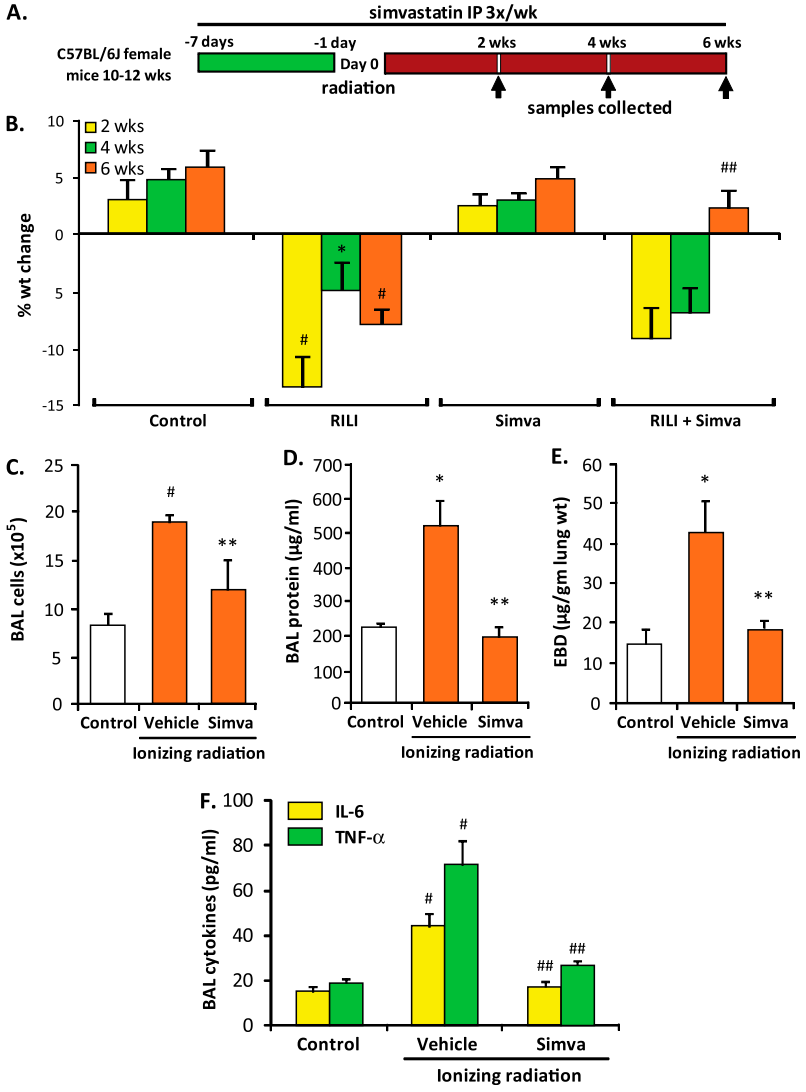

Figure 4. Protective effects of simvastatin treatment in murine RILI. (*A*) Mice received simvastatin (10 mg/kg body weight, 3×/wk) or vehicle beginning 1 week before radiation (25 Gy, single dose) and continuing up to 6 weeks after irradiation, with collection of BAL samples (protein, cell counts, biomarkers) and tissue (EBD, microarray, histology) at the interval indicated. (*B*) Simvastatin (Simva) treatment of irradiated mice resulted in significantly increased body weight at 6 weeks compared with irradiated controls ($n = 5$ animals/experimental group; $^{\#\#}P < 0.01$ compared with RILI alone), whereas radiation exposure alone produced significant weight loss at 2, 4, and 6 weeks ($^{*}P < 0.05$ and $^{\#}P < 0.01$ compared with controls). In addition, simvastatin attenuated radiation-induced increases in BAL cell counts (*B*) and both BAL protein (*C*) and EBD extravasation (*E*) at 6 weeks ($n = 5$ animals/experimental group; $^{*}P < 0.05$ and $^{\#}P < 0.01$ compared with controls; $^{**}P < 0.05$ compared with RILI alone). Earlier, at 4 weeks after irradiation, simvastatin treatment was associated with a significant reduction in BAL proinflammatory cytokines, TNF-α and IL-6 (*F*) ($n = 5$ animals/experimental group; $^{\#}P < 0.01$ compared with controls and $^{\#\#}P < 0.01$ compared with radiation alone).

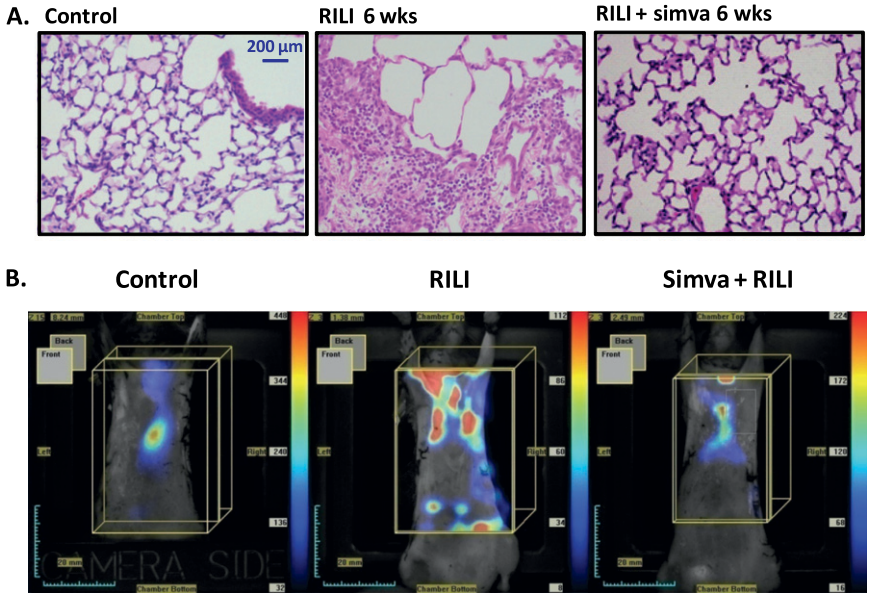

Figure 5. Effects of simvatatin on murine RILI lung histology and ViSen FMT imaging. (*A*) Significant attenuation of murine RILI and inflammatory cell infiltration in lungs from animals treated with simvastatin is apparent at 6 weeks after irradiation. (*B*) Simvastatin-treated RILI mice (25Gy) and control RILI mice (6 wk after irradiation) were injected with an intravascular, nontargeted blood pool probe (angiosense^{680}) and imaged (ViSen FMT imaging) at 24 hours after angiosense injection, allowing the extent of lung leakiness and injury to be quantified as fluorescent intensity. Control mice demonstrate dye retention in the vasculature (*yellow box*), whereas untreated RILI mice illustrate vascular leak by the extravasation of dye into the lung parenchyma. Simvastatin treatment of RILI mice significantly decreases dye extravasation, confirming the vascular barrier protective effects of simvastatin.

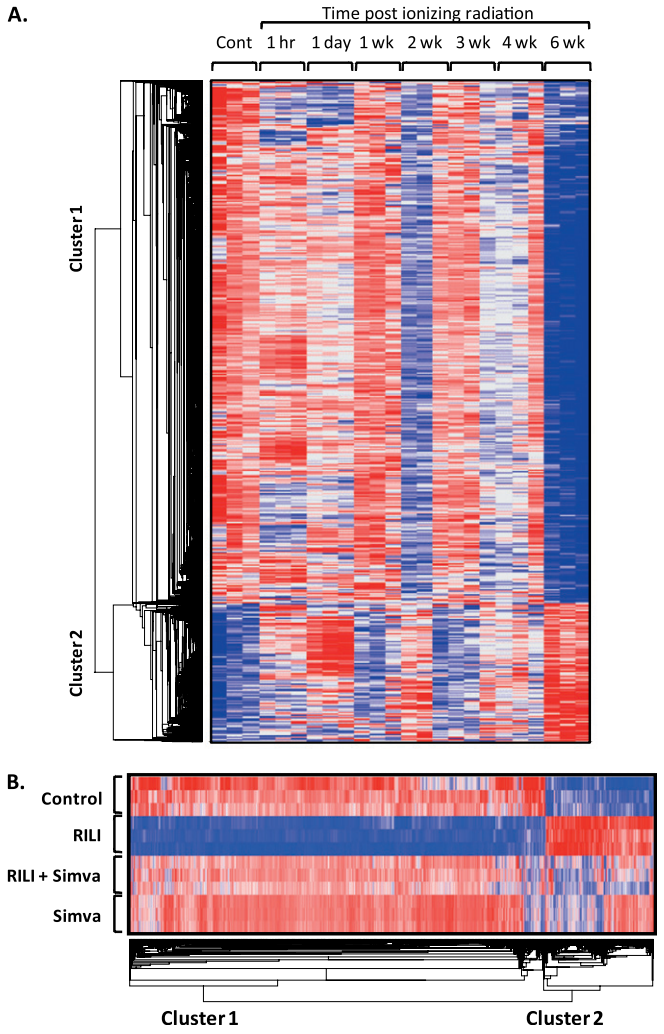

Figure 6. Dynamic changes in radiation-induced lung gene dysregulation. (*A*) The dysregulated genes at 6 weeks in RILI mice were identified by Significant Analysis of Microarrays (SAM) (Table E1, gene list 1). Expression levels across multiple time points after RILI were clustered and displayed by dChip software. Red, white and blue color indicates expression level above, at or below the average level of corresponding gene, respectively. (*B*) Hierarchical clustering of differentially expressed genes (control versus RILI) across all 6-week samples identified by significance analysis of microarrays (Table E1). Genes were displayed by dChip software, classified into two clusters (down-regulated genes, cluster 1; up-regulated genes, cluster 2). *Blue*, *white*, and *red colors* represent expression levels below, at, and above the average level of the corresponding gene, respectively.

Increased Histologic Inflammation and Lung Nitrotyrosine Expression in Murine RILI

Compared with control lungs, hematoxylin and eosin staining of murine lung sections showed considerable damage to type I pneumocytes at 4 weeks after irradiation (25 Gy), without visible edema or inflammation (Figure 3A). Lungs from mice at 6 weeks after irradiation exhibited modest alveolar flooding and inflammatory foci in scattered areas, with perivascular clustering of inflammatory cells prominent at 8 and 12 weeks. To investigate mechanisms involved in RILI, we assessed nitrotyrosine expression, a marker of peroxynitrite generation and RILI-induced oxidant injury (18). Nitrotyrosine expression was confined to lung epithelium, endothelium, and alveolar macrophages and, similar to BAL cytokine levels, peaked at 4 weeks (Figure 3B), but then declined to control levels 12 weeks after irradiation, despite increasing evidence of histologic injury (data not shown).

Protective Effects of Simvastain in a Preclinical Model of RILI

As lung inflammation and sustained alveolar barrier dysfunction are prominent features in murine RILI pathobiology, we next assessed the effects of simvastatin, an effective anti-inflammatory and lung edema–reducing pharmacological agent (12), on murine RILI. Simvastatin (10 mg/kg) was administered before irradiation (25 Gy), and weekly thereafter (three intraperitoneal injections per week for 6 wk) (Figure 4A). Simvastatin significantly attenuated radiation-induced weight loss (Figure 4B), increases in BAL inflammatory cells (Figure 4C), and both alveolar and lung vascular leak, as assessed by BAL protein levels (Figure 4D) and EBD extravasation (Figure 4E), respectively. In addition, proinflammatory cytokine levels were significantly reduced in the BAL fluid of simvastatin-treated animals compared with radiated controls (Figure 4F). These findings were corroborated by findings on lung histology as alterations in lung architecture, characterized by edema formation and lung inflammation associated with considerable type I pneumocyte damage, were markedly reduced in the lungs of simvastatin-treated animals (Figure 5A). We next performed lung imaging studies with assessment of RILI-induced extravasation of an intravascular probe (angiosense^{680}), which further confirmed the protective effects of simvastatin evidenced by an attenuation of probe signal throughout the lungs of radiation mice treated with simvastatin compared with irradiated controls (Figure 5B).

Deregulation of Gene Expression and Biological Pathways Induced by RILI and Attenuated by Simvastatin

Expression profiling of murine lung tissues (Affymetrix Mouse Genome 430 2.0 Array) to define RILI-driven genomic elements revealed robust radiation-induced differential lung gene expression, which was reversed by simvastatin (Table E1). The clustered heat map of radiation-induced dysregulated genes across all time points revealed that only a small subgroup of genes was dysregulated in the early phase after radiation (1 h and 1 d), whereas the majority of gene dysregulation occurred as unique, late-phase changes (6 wk after irradiation; Figure 6A). Simvastatin normalized radiation-mediated transcriptional suppression (Figure 6B), which was evidenced by the greater number of radiation-induced down-regulated genes (2,547 down-regulated genes) compared with up-regulated genes (677 up-regulated genes; Table E1). These findings were validated by GO analysis, which revealed that five of the seven major radiation-inhibited biological processes were related to transcriptional regulation or processing (transcription, mRNA processing, DNA-dependent regulation of transcription, chromatin modification, and RNA splicing), and were reversed by simvastatin (Table E2).

Radiation-deregulated genes were used to generate an "interactome" of proteins, which identified four genes/proteins (CD44, Cdc2a, spleen tyrosine kinase [Syk], Ccna2) as hubs for RILI-influenced protein–protein networks (Figure 7A). A PubMed database blast (PubMatrix) to determine the number of citations involving prioritized RILI interactome gene/protein components confirmed that greater than 50% of interactome components are associated with normal cellular responses to radiation (Table E3). GO enrichment analysis revealed simvastatin normalization of radiation-induced down-regulation of the focal adhesion pathway (seven genes), highly relevant to regulation of lung barrier integrity (Figure 7B), and ingenuity pathway analysis of up-regulated RILI genes revealed robust

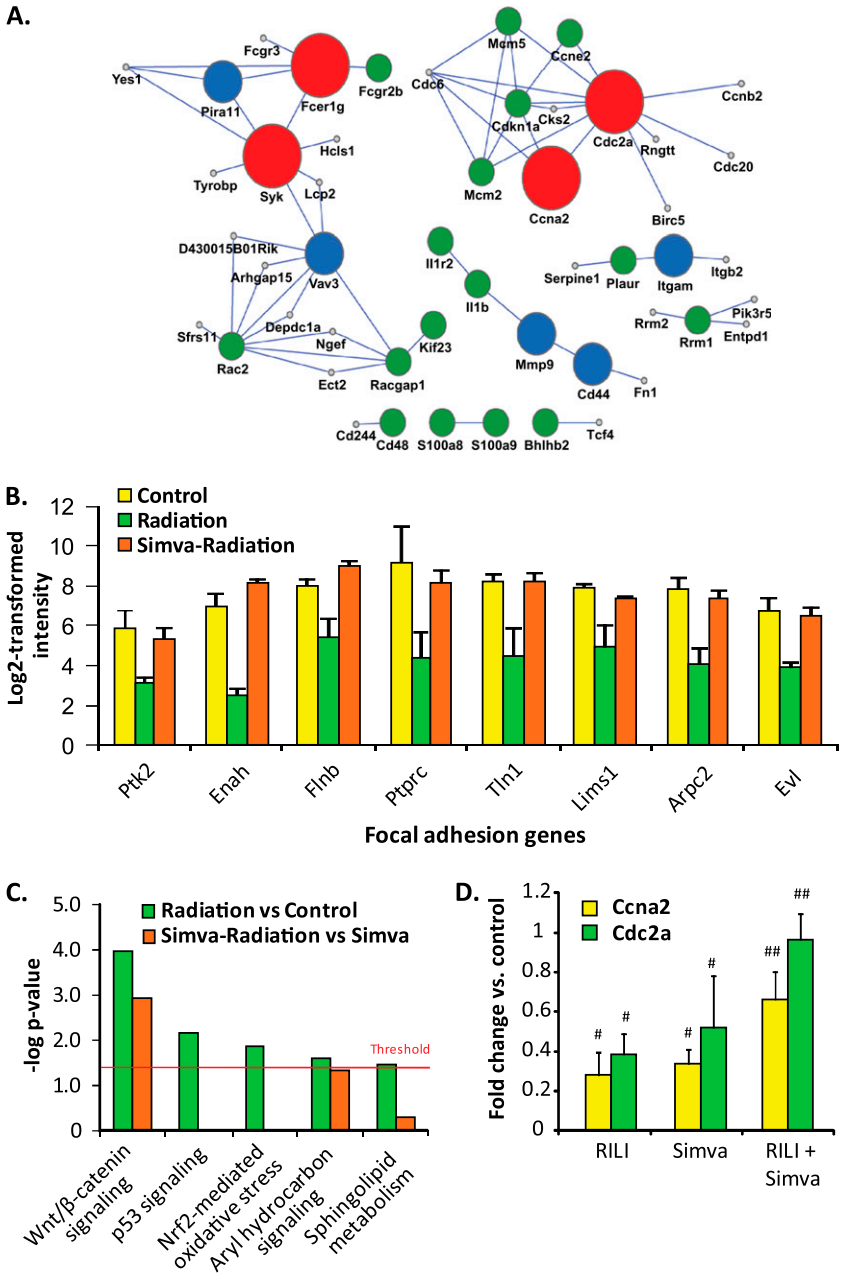

Figure 7. Radiation-mediated gene deregulation and biological pathways: attenuation by simvastatin. (*A*) Radiation-induced deregulated proteins identified by single network analysis of proteins (SNAP), a protein–protein interaction network analysis that identifies key deregulated interactors in simvastatin-treated radiated lungs using deregulated gene expression (Table E1) and network topology. False discovery rates were 0.0001% (*large red circles*), 5% (*medium-sized blue circles*), and 10% (*small green circles*). (*B*) Focal adhesion pathway genes are all significantly deregulated by RILI, and attenuated by simvastatin (Benjamini-Hochberg–corrected hypergeometric $P = 0.0035$). (*C*) Canonical pathways deregulated by irradiation in vehicle- and simvastatin-treated animals (*yellow* and *green*, respectively). Up-regulated genes were uploaded into Ingenuity Pathway Analysis software to identify overrepresented canonical pathways. Significance is determined by the single-sided Fisher's exact test at a *P* value of less than 0.05, as indicated by the *red threshold line* in the *graph*. (*D*) Real-time quantitative PCR validation of fold change in expression of deregulated Ccna2 and Cdc2 genes (RNA isolated from lung homogenates) after exposure to radiation, simvastatin, or both exposures. Ccna2 and Cdc2 were identified by SNAP, a protein–protein interaction network analysis used to identify most deregulated protein networks in radiated and simvastatin-treated lungs using the signature genes (Table E1, gene list 3), network topology, and expression dynamics family. The significance of gene dysregulation is determined by two-group comparison using a *t* test. Radiation exposure reduces expression of both of Ccna2 and Cdc2, whereas simvastatin treatment reverses this reduction with increased expression of both genes ($^{\#\#}P = 0.01$ compared with radiated controls).

activation of five canonical pathways (wnt/β-catenin, p53, aryl hydrocarbon receptor, nuclear factor–erythroid-2–related factor (Nrf) 2 signaling, and sphingolipid metabolism), with each deregulated pathway either attenuated or completely reversed by simvastatin (Figure 7C). Finally, radiation-mediated transcriptional inhibition of the cell cycle genes, Cdc2 and Ccna2, was validated by RT-PCR (Figure 7D), with the inhibition reversed by simvastatin.

DISCUSSION

Our results suggest that simvastatin may serve as a novel alternative to aggressive corticosteroid therapy in RILI, a potentially fatal complication of radiotherapy and a substantial treatment limitation for the hundreds of thousands patients worldwide receiving radiotherapy for thoracic malignancies. Simvastatin was selected for these studies due to the known anti-inflammatory and alveolar and vascular barrier–protective properties of statins. Via altered small GTPase signaling to the cytoskeleton (12), simvastatin markedly reduced multiple RILI inflammatory indices, including leukocyte infiltration and lung permeability, consistent with prior studies in rodent models of LPS-induced acute lung injury (12), ischemia–reperfusion injury (19), and pulmonary hypertension (20). Although the protective effects of statins in animal models of radiation injury have previously been investigated (21, 22), our studies are the first to characterize the lung vascular–protective effects of statins in RILI. Moreover, we report, for the first time, effects of statins on relevant radiation-induced dysregulation of lung gene expression, with subsequent protein–protein interaction network analysis. Simvastatin potently suppressed radiation-induced gene stress pathways (Wnt-β catenin-, Nrf2-, and p53-signaling pathways) via transcriptional reprogramming of radiation-dysregulated genes, findings compatible with reports of simvastatin-mediated down-regulation of chemokine and chemokine receptor expression (23), the expression of which on the endothelial surface is increased

by radiation (24). Quantitative and qualitative changes in RILI gene expression resulted in cytokine overproduction, which, in autocrine and paracrine fashion, increase mRNA translation (25), triggering a cascade leading to RILI pathobiology.

The striking paucity of mechanistic information that addresses RILI pathogenesis likely reflects the lack of appropriate preclinical animal models that mimic human RILI. Several lines of evidence suggest the validity and utility of our preclinical murine model of RILI for the interrogation of RILI pathobiology. Murine RILI followed a single clinically relevant radiation dose (18–25 Gy), and evolved in a dose- and time-dependent fashion (over 12 wk) with increased vascular leak and leukocyte infiltration. Notably, as the inflammatory indices we assessed (BAL cells, protein, EBD extravasation, and BAL cytokines) represent different aspects of the inflammatory response associated with RILI, the disparate kinetics are not surprising, given such a highly complex process. The decline in nitrotyrosine expression and BAL cytokine levels to control levels by 12 weeks after irradiation suggest that these elements contribute to early histological injury, but not to more delayed injury. In this regard, unlike other murine RILI models (21, 22, 26), our results may indicate a discordance between alveolar epithelial barrier function and vascular leakage, hallmarks of inflammatory lung injury and a phenotypic consequence of RILI (10), which we speculate to be linked to differential susceptibility of type I pneumocytes and vascular endothelium to ionizing radiation. Alveolar injury and barrier dysfunction was sustained at lower levels of radiation, and remained progressive over the 12 weeks of RILI, whereas radiation-induced vascular leakage occurred only with the highest radiation dose, and completely resolved by 12 weeks. Epithelial and endothelial injury and barrier dysfunction are facilitated by the increased levels of oxidative and nitrosative stress induced by direct ionizing radiation (18, 27, 28). Consistent with the increased Reactive Oxygen Species/Reactive Nitrogen Species (ROS/RNS) observed in our preclinical model, the Nrf2 pathway was prominently deregulated in RILI. Simvastatin normalized radiation-induced Nrf2 deregulation, which is essential for the coordinated induction of genes encoding stress-responsive and cytoprotective proteins (29, 30). Finally, compelling support for our preclinical RILI model was obtained by filtering RILI- and simvastatin-influenced deregulated genes as an interactome of RILI-deregulated proteins. These network-modeling studies identified CD44, Cdc2a, Syk, and Ccna2 as key interactors, which are significantly altered by exposure to ionizing radiation. PubMatrix analysis verified the participation of these prioritized genes in cellular responses to radiation, whereas the paucity of citations linked to radiation pneumonitis or RILI reflects the novelty of our approach. Although our results do not directly implicate the homologous human genes in the pathobiology of RILI, the available literature firmly supports their relevance in this context. For example, Cdc2a and Ccna2 function as checkpoint genes critical to radiation effects in tissues, and the cytoplasmic Syk functions as a tumor suppressor involved in responses to oxidative stress (31), including endothelial cells (32). CD44 is a key regulatory receptor for hyaluronan involved in responses to lung injury, including RILI (26, 33), and regulation of vascular permeability (34).

In summary, we have used multidimensional approaches to establish and validate a murine model of RILI, which exhibits temporal increases in lung permeability, leukocyte influx, and proinflammatory cytokine secretion—findings compatible with the limited reports of human and murine models of thoracic irradiation (22). Moreover, we validated the profound clinical promise of simvastatin as a protective strategy to attenuate the untoward effects of RILI. Given the availability, affordability, and favorable safety profile of this class of drugs, simvastatin-like drugs may potentially allow for radiation dose escalation, while enhancing outcomes of patients receiving radiotherapy for thoracic malignancies.

Author Disclosure: C.T.C. has received a National Institutes of Health (NIH)–sponsored grant (more than $100,000) for research; S.M.D. has received an NIH-sponsored grant (more than $100,000) for research; V.N. has received an NIH-sponsored grant (more than $100,000) for research; Y.A.L. has three patents with Columbia University (Provisional Patent Application: Methods for extracting phenotypic information from the literature via natural language processing, U.S. Patent 20060074991—System and method for generating an amalgamated database. Clinigene. International Patent Application PCT/US03/35470; and Terminological Mapping. Continuation-in-Part of International Patent Application (PCT/US03/35470), and also has a patent with Memorial Sloan Kettering Cancer Center (U.S. Patent 7528116, Kinase suppressor of Ras inactivation for therapy of Ras-mediated tumorigenesis); none of the other authors has a financial relationship with a commercial entity that has an interest in the subject of this manuscript.

Acknowledgments: The authors express gratitude to Eddie T. Chiang and Carrie L. Evenoski for superb technical assistance.

References

1. Vujaskovic Z, Marks LB, Anscher MS. The physical parameters and molecular events associated with radiation-induced lung toxicity. *Semin Radiat Oncol* 2000;10:296–307.
2. Carruthers SA, Wallington MM. Total body irradiation and pneumonitis risk: a review of outcomes. *Br J Cancer* 2004;90:2080–2084.
3. Roberts CM, Foulcher E, Zaunders JJ, Bryant DH, Freund J, Cairns D, Penny R, Morgan GW, Breit SN. Radiation pneumonitis: a possible lymphocyte-mediated hypersensitivity reaction. *Ann Intern Med* 1993; 118:696–700.
4. Rodrigues G, Lock M, D'Souza D, Yu E, Van Dyk J. Prediction of radiation pneumonitis by dose–volume histogram parameters in lung cancer—a systematic review. *Radiother Oncol* 2004;71:127–138.
5. Travis EL. Early indicators of radiation injury in the lung: are they useful predictors for late changes? *Int J Radiat Oncol Biol Phys* 1980; 6:1267–1269.
6. Kwok E, Chan CK. Corticosteroids and azathioprine do not prevent radiation-induced lung injury. *Can Respir J* 1998;5:211–214.
7. Molteni A, Moulder JE, Cohen EF, Ward WF, Fish BL, Taylor JM, Wolfe LF, Brizio-Molteni L, Veno P. Control of radiation-induced pneumopathy and lung fibrosis by angiotensin-converting enzyme inhibitors and an angiotensin ii type 1 receptor blocker. *Int J Radiat Biol* 2000;76:523–532.
8. Ware LB, Matthay MA. The acute respiratory distress syndrome. *N Engl J Med* 2000;342:1334–1349.
9. Dudek SM, Garcia JG. Cytoskeletal regulation of pulmonary vascular permeability. *J Appl Physiol* 2001;91:1487–1500.
10. Gross NJ. Experimental radiation pneumonitis. IV. Leakage of circulatory proteins onto the alveolar surface. *J Lab Clin Med* 1980;95: 19–31.
11. Undas A, Brozek J, Musial J. Anti-inflammatory and antithrombotic effects of statins in the management of coronary artery disease. *Clin Lab* 2002;48:287–296.
12. Jacobson JR, Barnard JW, Grigoryev DN, Ma SF, Tuder RM, Garcia JG. Simvastatin attenuates vascular leak and inflammation in murine inflammatory lung injury. *Am J Physiol Lung Cell Mol Physiol* 2005; 288:L1026–L1032.
13. Moitra J, Evenoski C, Sammani S, Wadgaonkar R, Turner JR, Ma SF, Garcia JG. A transgenic mouse with vascular endothelial over-expression of the non-muscle myosin light chain kinase–2 isoform is susceptible to inflammatory lung injury: role of sexual dimorphism and age. *Transl Res* 2008;151:141–153.
14. Moitra J, Sammani S, Garcia JG. Re-evaluation of evans blue dye as a marker of albumin clearance in murine models of acute lung injury. *Transl Res* 2007;150:253–265.
15. Hong SB, Huang Y, Moreno-Vinasco L, Sammani S, Moitra J, Barnard JW, Ma SF, Mirzapoiazova T, Evenoski C, Reeves RR, *et al.* Essential role of pre–B-cell colony enhancing factor in ventilator-induced lung injury. *Am J Respir Crit Care Med* 2008;178:605–617.
16. Meyer NJ, Huang Y, Singleton PA, Sammani S, Moitra J, Evenoski CL, Husain AN, Mitra S, Moreno-Vinasco L, Jacobson JR, *et al.* Gadd45a is a novel candidate gene in inflammatory lung injury via influences on akt signaling. *FASEB J* 2009;23:1325–1337.

17. Tusher VG, Tibshirani R, Chu G. Significance analysis of microarrays applied to the ionizing radiation response. *Proc Natl Acad Sci USA* 2001;98:5116–5121.
18. Giaid A, Lehnert SM, Chehayeb B, Chehayeb D, Kaplan I, Shenouda G. Inducible nitric oxide synthase and nitrotyrosine in mice with radiation-induced lung damage. *Am J Clin Oncol* 2003;26:e67–e72.
19. Moreno-Vinasco L, Jacobson JR, Bonde P, Sammani S, Mirzapoiazova T, Vigneswaran WT, Garcia JGN. Attenuation of rodent lung ischemia–reperfusion injury by sphingosine 1-phosphate. *J Org Dysfunc* 2008;4:106–114.
20. Girgis RE, Li D, Zhan X, Garcia JG, Tuder RM, Hassoun PM, Johns RA. Attenuation of chronic hypoxic pulmonary hypertension by simvastatin. *Am J Physiol Heart Circ Physiol* 2003;285: H938–H945.
21. Ostrau C, Hulsenbeck J, Herzog M, Schad A, Torzewski M, Lackner KJ, Fritz G. Lovastatin attenuates ionizing radiation–induced normal tissue damage in vivo. *Radiother Oncol* 2009;92:492–499.
22. Williams JP, Hernady E, Johnston CJ, Reed CM, Fenton B, Okunieff P, Finkelstein JN. Effect of administration of lovastatin on the development of late pulmonary effects after whole-lung irradiation in a murine model. *Radiat Res* 2004;161:560–567.
23. Jacobson JR, Dudek SM, Birukov KG, Ye SQ, Grigoryev DN, Girgis RE, Garcia JG. Cytoskeletal activation and altered gene expression in endothelial barrier regulation by simvastatin. *Am J Respir Cell Mol Biol* 2004;30:662–670.
24. Kureishi Y, Luo Z, Shiojima I, Bialik A, Fulton D, Lefer DJ, Sessa WC, Walsh K. The HMG-CoA reductase inhibitor simvastatin activates the protein kinase akt and promotes angiogenesis in normocholesterolemic animals. *Nat Med* 2000;6:1004–1010.
25. Lu X, de la Pena L, Barker C, Camphausen K, Tofilon PJ. Radiation-induced changes in gene expression involve recruitment of existing messenger RNAs to and away from polysomes. *Cancer Res* 2006;66: 1052–1061.
26. Iwakawa M, Noda S, Ohta T, Oohira C, Tanaka H, Tsuji A, Ishikawa A, Imai T. Strain dependent differences in a histological study of CD44 and collagen fibers with an expression analysis of inflammatory response–related genes in irradiated murine lung. *J Radiat Res (Tokyo)* 2004;45:423–433.
27. Hallahan DE, Virudachalam S, Kuchibhotla J. Nuclear factor kappaB dominant negative genetic constructs inhibit X-ray induction of cell adhesion molecules in the vascular endothelium. *Cancer Res* 1998;58: 5484–5488.
28. Zhao W, Robbins ME. Inflammation and chronic oxidative stress in radiation-induced late normal tissue injury: therapeutic implications. *Curr Med Chem* 2009;16:130–143.
29. Dinkova-Kostova AT, Talalay P. Direct and indirect antioxidant properties of inducers of cytoprotective proteins. *Mol Nutr Food Res* 2008; 52:S128–S138.
30. Cho HY, Reddy SP, Kleeberger SR. Nrf2 defends the lung from oxidative stress. *Antioxid Redox Signal* 2006;8:76–87.
31. Qin S, Kurosaki T, Yamamura H. Differential regulation of oxidative and osmotic stress induced SYK activation by both autophosphorylation and SH2 domains. *Biochemistry* 1998;37:5481–5486.
32. Foncea R, Carvajal C, Almarza C, Leighton F. Endothelial cell oxidative stress and signal transduction. *Biol Res* 2000;33:89–96.
33. Sakai M, Iwakawa M, Iwakura Y, Ohta T, Tsujii H, Imai T. Cd44 and bak expression in IL-6 or TNF-alpha gene knockout mice after whole lung irradiation. *J Radiat Res (Tokyo)* 2008;49:409–416.
34. Singleton PA, Salgia R, Moreno-Vinasco L, Moitra J, Sammani S, Mirzapoiazova T, Garcia JG. CD44 regulates hepatocyte growth factor–mediated vascular integrity: role of c-Met, Tiam1/Rac1, dynamin 2, and cortactin. *J Biol Chem* 2007;282:30643–30657.